Published in final edited form as:
Lab Invest. 2016 June ; 96(6): 623–631. doi:10.1038/labinvest.2016.40.

Secretory leukocyte protease inhibitor gene deletion alters bleomycin-induced lung injury, but not development of pulmonary fibrosis

Anthony N Habgood[1], **Amanda L Tatler**[1], **Joanne Porte**[1], **Sharon M Wahl**[2], **Geoffrey J Laurent**[3], **Alison E John**[1], **Simon R Johnson**[1], and **Gisli Jenkins**[1]

[1]Nottingham Respiratory Research Unit, University of Nottingham, Nottingham, England [2]National Institute of Dental & Craniofacial Research, NIH, Bethesda, Maryland, USA [3]Lung Institute of Western Australia, The University of Western Australia, Perth, Australia

Abstract

Idiopathic Pulmonary Fibrosis (IPF) is a progressive, fatal disease with limited treatment options. Protease mediated transforming growth factor-β (TGF-β) activation has been proposed as a pathogenic mechanism of lung fibrosis. Protease activity in the lung is tightly regulated by protease inhibitors, particularly secretory leukocyte protease inhibitor (SLPI). The bleomycin model of lung fibrosis was used to determine the effect of increased protease activity in the lungs of *Slpi*$^{-/-}$ mice following injury. *Slpi*$^{-/-}$, and wild-type, mice received oropharyngeal administration of bleomycin (30 IU) and the development of pulmonary fibrosis was assessed. Pro and active forms of matrix metalloproteinase-2 (MMP-2) and MMP-9 were measured. Lung fibrosis was determined by collagen subtype specific gene expression, hydroxyproline concentration, and histological assessment. Alveolar TGF-β activation was measured using bronchoalveolar lavage cell pSmad2 levels and global TGF-β activity was assessed by pSmad2 immunohistochemistry. The active-MMP-9 to pro-MMP-9 ratio was significantly increased in *Slpi*$^{-/-}$ animals compared with wild-type animals, demonstrating enhanced metalloproteinase activity. Wild-type animals showed an increase in TGF-β activation following bleomycin, with a progressive and sustained increase in collagen type I, alpha 1 (*Col1α1*), III, alpha 1(*Col3α1*), IV, alpha 1(*Col4α1*) mRNA expression, and a significant increase in total lung collagen 28 days post-bleomycin. In contrast *Slpi*$^{-/-}$ mice showed no significant increase of alveolar TGF-β activity following bleomycin, above their already elevated levels, although global TGF-β activity did increase. *Slpi*$^{-/-}$ mice had impaired collagen gene expression but animals demonstrated minimal

Corresponding author Mr Anthony Habgood, Nottingham Respiratory Research Unit, University of Nottingham, Nottingham University Hospitals, Clinical Sciences Building, City Hospital Campus, Nottingham, NG5 1PB, UK. anthony.habgood@nottingham.ac.uk. Telephone: (+44) 0115 82 31106.

DISCLOSURES

Dr Gisli Jenkins has Sponsored Research Grants from GlaxoSmithKline, Novartis and Biogen Idec. He has undertaken consultancy work for GlaxoSmithKline, Boehringer Ingelheim, PharmAkea Therapeutics, Roche, Biogen Idec and Intermune and has received lecture fees from MedImmune.

Supplementary information is available at Laboratory Investigation's website.

Europe PMC Funders Author Manuscripts

reduction in lung fibrosis compared with wild-type animals. These data suggest that enhanced proteolysis does not further enhance TGF-β activation, and inhibits sustained *Col1α1*, *Col3α1* and *Col4α1* gene expression following lung injury. However, these changes do not prevent the development of lung fibrosis. Overall, these data suggest that the absence of *Slpi* does not dramatically modify the development of lung fibrosis following bleomycin-induced lung injury.

Idiopathic pulmonary fibrosis (IPF) is a fibroproliferative disorder that leads to architectural remodelling of the lung with detrimental effects on pulmonary function. It is a chronic, progressive disease with limited therapeutic options and the prognosis remains very poor with a median survival of around 3 years (1). The aetiology and underlying pathophysiology of IPF remain unclear. The current paradigm suggests that injury to the alveolar epithelium leads to an exaggerated or dysregulated fibrotic response (2, 3). Whilst the role of inflammation in the pathogenesis of IPF remains controversial, neutrophilic polymorphonuclear leukocytes (neutrophils, PMNs) have been associated with severe, progressive fibrosis (4).

Neutrophil granules contain serine proteases such as neutrophil elastase (NE), cathepsin G (CAT G) and proteinase-3 (PR-3). These granular contents are released in large quantities from activated neutrophils (5) and their substrates include most matrix proteins, particularly elastin, and, to a lesser extent, collagen, laminin, fibronectin and vitronectin (6). Neutrophil proteases have been implicated in pulmonary fibrosis. Both *Ne*$^{-/-}$ mice and animals treated with inhibitors of NE are resistant to bleomycin (BLM)-induced pulmonary fibrosis (7-9). Furthermore, levels of NE are increased in both bronchoalveolar lavage (BAL) fluid and the lung parenchyma (10, 11) from patients with IPF. The mechanism through which proteases promote fibrosis remains unclear, although serine proteases have been shown to activate transforming growth factor-β (TGF-β) directly via proteolytic cleavage of the latency associated peptide (LAP) *in vitro* (12-14) and indirectly through activation of αv containing integrins (15, 16).

Protease activity in the lung is regulated by a number of protease inhibitors. Secretory leukocyte protease inhibitor (SLPI) is an 11.7kDa protein containing a protease inhibitory site located at leucine 72 in the carboxy-terminal domain (17). SLPI is predominately secreted by epithelial cells (18) and in the absence of SLPI, elastolytic activity in dermal and mucosal wounds has been shown to be enhanced resulting in enhanced active TGF-β, prolonged wound repair and increased scarring (19, 20), suggesting that proteases may activate TGF-β and promote fibrosis (19).

This study aims to determine the role of SLPI regulated protease activation on the development of pulmonary fibrosis. Wild-type mice had an increase in collagen gene expression, total lung collagen and phosphorylation of Smad2 28 days following bleomycin instillation, whereas *Slpi*$^{-/-}$ mice had evidence of increased metalloproteinase activity and more severe acute injury. However, increases in collagen gene expression in *Slpi*$^{-/-}$ mice were not sustained over 28 days and animals demonstrated minimal reduction in lung fibrosis compared with wild-type animals. These data suggest that enhanced proteolysis in *Slpi*$^{-/-}$ mice may promote acute lung injury however this ultimately has little effect on the severity of fibrosis when compared with wild-type animals.

Europe PMC Funders Author Manuscripts

MATERIALS AND METHODS

Animals

Slpi$^{-/-}$ mice on a B6D2F1 background were kindly donated by Sharon Wahl (19). This recombinant strain is now available at The Jackson Laboratory Repository with JAX Stock No. 010926 (http://jaxmice.jax.org/query). C57Bl6/j mice were obtained from Charles River UK (Margate, Kent, U.K.). *Slpi*$^{-/-}$ mice were backcrossed by mating with C57Bl6/j for at least five generations within the Biomedical Services Unit, University of Nottingham. Animals had free access to food (Tekland Global 18 % protein rodent diet; Bicester, Oxen, U.K.) and water. Ear notch biopsies from animals were analyzed by polymerase chain reaction (PCR). The presence of the *Slpi* allele was detected by primers: sense - 5′-CAAGGCCTTCTGTGTGTAACTTTC -3′ and antisense - 5′-CTGCTACAGAGTAGGTGGCAGAC -3′, resulting in a 490-bp PCR product and the Neo cassette allele by primers: sense - 5′- CGCTTCCTCGTGCTTTACGGTATC -3′ and antisense - 5′- GATGCCAGGCATTTGCACTGCCG -3′, resulting in a 344-bp product.

Bleomycin model

All animal care and procedures were approved by the University of Nottingham Ethical Review Committee and were performed under Home Office Project and Personal License authority within the Animal (Scientific Procedures) Act 1986. Mice, 6-8 weeks old, were anaesthetized with isoflurane-anaesthetic and exposed to 30 IU of bleomycin sulphate (Kyowa Hakko, Slough, UK) in 50 μl sterile 0.9 % saline (Sigma Aldrich), or 50 μl sterile 0.9 % saline control, via oropharyngeal administration (*o.p.*).

Histology

28 days post-bleomycin the trachea was cannulated and the pulmonary vasculature perfused with 10 ml of heparinized PBS (40 U/ml) via the pulmonary artery. Lungs were inflated with formalin under set constant gravitational pressure (20 cm H_2O), and the lungs removed *en bloc* and fixed in 10 ml of formalin. Fixed tissues were embedded in paraffin wax prior to sections 5 μm thick being cut, rehydrated in graded alcohol and stained by Masson's trichrome. Severity of lung fibrosis was quantified through Ashcroft scoring (21) of Masson's trichrome stained tissue sections.

Immunohistochemistry

5 μm thick lung tissue sections were deparaffinized in xylene and rehydrated in graded ethanol. Antigen retrieval was performed via heating sections in 10 mM sodium citrate buffer (pH6.0) in a microwave for 10 min. Subsequently, endogenous peroxidase activity was blocked by incubating sections in 3 % H_2O_2 in methanol for 30 min. Nonspecific antibody binding was blocked using goat serum (Sigma Aldrich) for 30 min, prior to incubation with human anti-mouse collagen type I (ab292) (2 μg/ml), III (ab7778) (1 μg/ml), IV (ab6586) (0.5 μg/ml), VI (6588) (0.5 μg/ml) (Abcam, Cambridge, UK), or rabbit anti-mouse Phospho-Smad2 (#3101) (1:2000 dilution) primary antibody (Cell Signaling Technology, Inc., Boston, MA, USA) overnight at 4 °C. Sections were then incubated with a biotin-conjugated secondary antibody. Biotin-conjugated secondary antibody was detected

through incubation with an avidin/biotinylated enzyme complex (ABC) solution (Vector Laboratories) for 30 min; colour development was performed using 3,3′-diaminobenzidine tetrahydrochloride (Sigma Aldrich). Sections were counterstained using Mayer's hematoxylin and visualized under a Nikon 90i light microscope. The total area of collagen I, III, IV and VI, positively stained tissue, in fibrotic lesions greater than 7 500 μm^2, was measured using NIS-Elements (Nikon instruments). A single cross section from all five lung lobes, per mouse, were analysed and total area of positively stained collagen was calculated as a percentage of total lung tissue area.

Analysis of lung collagen content

Lungs were removed and immersed immediately in liquid nitrogen prior to storage at −80 °C. Lung tissue was ground to a fine powder under liquid nitrogen. Ground lung tissue was mixed in 1 ml distilled water on ice in Pyrex® tubes and incubated in 125 μl 50 % TCA (Sigma Aldrich) at 4 °C for 20 min. Samples were centrifuged at 528 × g for 10 min at 4 °C. The lungs were then hydrolyzed in 1 ml of 12 N HCL overnight at 110 °C prior to reconstitution in 2 ml of distilled water. 200 μl of hydrozylate, or hydroxyproline standard (Sigma Aldrich), were oxidized in 500 μl chloramine T (Sigma Aldrich) for 20 min at room temperature (RT) prior to the addition of 500 μl of Ehrlich's solution (Sigma Aldrich) and incubation at 65 °C for 15 min. Samples were then incubated at RT for 2 hours prior to colorimetric analysis at an absorbance of 550 nm. Hydroxyproline per mg of lung tissue was calculated against a standard curve.

RT-PCR

RNA was isolated from frozen lung tissue using a TRIzol® based extraction protocol. RNA (2 μg) was reverse transcribed using moloney murine leukemia virus reverse transcriptase (Promega) to produce cDNA for real time polymerase chain reaction (RT-PCR) analysis. Primers used: *Slpi* forward - 5′-GCTGTGAGGGTATATGTGGGAAA-3′ and reverse - 5′-CGCCAATGTCAGGGATCAG-3′, *Mmp-9* forward - 5′-TGAATCAGCTGGCTTTTGTG-3′ and reverse - 5′-GTGGATAGCTCGGTGGTGTT-3′, *Col1a1* forward - 5′-GGAGGGCGAGTGCTGTGCTTT-3′ and reverse, 5′-GGGACCAGGAGGACCAGGAAGT-3′, *Col3a1* forward - 5′-AGGTACCGATTTGAACAGGCT-3′ and reverse, 5′- TTTGCAGCCTGGGCTCATTT -3′, *Col4a1* forward - 5′-AAGCCCATTCCTCCAACTGA-3′ and reverse - 5′-AAGGACAAATCGGACCCACT-3′, *Col6a1* forward - 5′-GATGAGGGTGAAGTGGGAGA-3′ and reverse, 5′-CAGCACGAAGAGGATGTCAA-3′. Amplification was performed using an MXPro3000 QPCR system (Stratagene). Kapa Taq polymerase (Kapa Biosystems) was activated at 95 °C for 3 min followed by 40 cycles of denaturing, annealing and extension (95 °C 30 seconds, 60 °C 30 seconds and 72 °C 20 seconds respectively). Annealing was conducted at 59 °C for *Col6a1*. Ct values were standardized to a housekeeper gene, hypoxanthine-guanine phosphoribosyltransferase (HPRT): forward - 5′-TGAAAGACTTGCTCGAGATGTCA-3′ and reverse - 5′-CCAGCAGGTCAGCAAAGAACT-3′. Amplification of a single DNA product was confirmed by melting curve analysis. Data expressed as mean relative expression using the $\Delta\Delta C_t$ equation as described previously (22).

Zymography

MMP-2 and MMP-9 activity was assessed via gelatin zymography. 10 μl of BAL supernatant was diluted 1:1 in Tris-Gly SDS zymogram samples buffer (Invitrogen), and incubated at 21 °C for 10 min. 15 μl of sample (or standard) was loaded onto zymogram precast gelatin gels, 10 % Tris-Glycine gel with 0.1 % gelatin substrate (Invitrogen) and subjected to electrophoresis at constant voltage of 125 V for 100 min. Gels were incubated at RT for 60 min in 100 ml of zymogram renaturing buffer, 2.5 % Triton X-100 (Invitrogen), to recover enzymatic activity. Gels were then incubated in zymogram developing buffer, 50 mM Tris-HCl, pH 7.5, 200 mM NaCl, 5 mM $CaCl_2$ (Invitrogen) for 1 hour prior to overnight incubation at 37 °C. Gels were then stained with coomassie blue-stain (Coomassie blue 0.1 % (w/v) in H_2O 50 % (v/v), methanol 40 % (v/v) and acetic acid 10 % (v/v)) for 60 min before destaining in the same solution without the dye for 30 min. Bands were then visualized by image analysis (Gel Doc, Syngene, Cambridge, UK) and densitometry determined using Image J software. Band densities were standardized to the mean density of two control samples, per gel, to allow comparisons between multiple gels. All gels were run in parallel.

Macrophage TGF-β activity

Nuclear fraction of BAL cells was extracted, 28 days post-bleomycin treatment, using a nuclear extraction kit (Active-motif). Briefly, lungs were lavaged with a total of 4.5 ml of PBS containing phosphatase inhibitor (Active-motif). Cells were pelleted via centrifugation at 528 × g for 10 min (4 °C) and the supernatant was removed and stored at −80 °C. Total cell pellets were re-suspended in 250 μl of hypotonic lysis buffer and incubated on ice for 15 min. 12.5 μl of detergent (Active-motif) was added and the samples were vortexed for 10 seconds prior to centrifugation for 1 minute at 14 000 × g (4 °C) and re-suspended in 25 μl of lysis buffer (Active-motif). Samples were vortexed and centrifuged for 1 min at 14 000 × g (4 °C) and the nuclear fraction removed for pSmad2 assessment using the PathScan® Total Smad2 Sandwich ELISA Kit (Cell Signaling Technology, Inc.). 10 μg of total cell nuclear protein was assayed from each sample.

Neutrophil elastase activity

28 days post-bleomycin treatment, lungs were excised and snap-frozen in liquid nitrogen prior to storage at −80 °C. Lung tissue was ground to a fine powder under liquid nitrogen and resuspended in 1 ml 0.1 M Tris pH 7.4. After 3 cycles of freezing and thawing, the lung lysates were centrifuged at 20 800 × g for 30 min at 4 °C. NE activity was measured in lung homogenate using the synthetic fluorescent, MeOSu-AAPV-AMC substrate (Santa-Cruz, Dallas, TX, USA). Lung homogenate (1.5 mg/ml protein concentration) was incubated with MeOSu-AAPV-AMC (0.1 nM final concentration) in 0.1 M Tris pH 7 (total volume 250 μl) in a black bottom/wall 96 well plate and the amount of NE released fluorescent product was determined at 2 hours. Plates were read using excitation 355 nm and 460 nm emission wavelengths; background fluorescence of the substrate only was subtracted from each sample.

Statistical analysis

All data are reported as mean ± SEM of *n* observations. Student's *t* test was used for comparison between two groups. Two-way ANOVA was used for comparison of multiple data sets. *P* values less than 0.05 were considered significant. All statistical analysis was performed using GraphPad Prism (v6.01, La Jolla, CA, USA).

RESULTS

Slpi gene deletion promotes a proteolytic environment in the lung

The genotype of *Slpi*$^{-/-}$ mice was confirmed by PCR (Figure 1a). *Slpi* mRNA was analysed in lung tissue by quantitative RT-PCR to confirm that *Slpi*$^{-/-}$ mice had *Slpi* deficiency in the lung (Figure 1b). To determine if *Slpi* deficiency altered serine proteinase activity NE activity was measured 28 days post-bleomycin, but no differences were detected regardless of genotype or injury (Figure 1c). Serine proteases can activate both MMP-2 and MMP-9 (23, 24), therefore the ratio of pro-MMP-2 and MMP-9 and active MMP-2 and MMP-9 was determined 28 days post-bleomycin (Figures 1d and e respectively; gelatin zymography gel images available in supplementary Figures S1a, b and c). There was no difference between levels of active MMP-2 and MMP-9 in saline exposed mice of either genotype. However, following bleomycin exposure, there was no increase in active MMP-2 (Figure 1d) but an increase in active MMP-9 in bleomycin exposed *Slpi*$^{-/-}$ mice, compared with either saline or wild-type controls ($P = 0.05$), was detected (Figure 1e). The effects of SLPI on active MMP-9 levels were not due to enhanced MMP-9 expression because no differences in *Mmp-9* mRNA levels were found between wild-type and *Slpi*$^{-/-}$ mice exposed to saline or bleomycin 28 days post-bleomycin (Figure 1f).

Bleomycin induced lung fibrosis does not enhance alveolar TGF-β activation in *Slpi*$^{-/-}$ mice, although they still develop pulmonary fibrosis

To determine the effect of *Slpi* gene deletion on the development of pulmonary fibrosis, macrophage TGF-β activation and lung histology in *Slpi*$^{-/-}$ mice were evaluated. Levels of nuclear pSmad2 from alveolar macrophages were significantly increased in wild-type mice 28 days post-bleomycin exposure compared with saline controls ($P = 0.003$; Figure 2a). In contrast, there was a trend towards increased basal pSmad2 in *Slpi*$^{-/-}$ mice but this was not significantly increased following bleomycin exposure (Figure 2a). Global tissue TGF-β activation was measured by pSmad2 immunostaining. In saline instilled mice there was evidence of increased pSmad2 staining in *Slpi*$^{-/-}$ mice around both the alveoli and larger airways (Figure 2b). Bleomycin treatment increased pSmad2 staining in both wild-type and *Slpi*$^{-/-}$ mice, primarily at areas of injury and fibroproliferation. Examination of lung sections from both wild-type, and *Slpi*$^{-/-}$, mice demonstrated areas of severe fibrosis following bleomycin exposure compared with saline controls (Figure 2c). The extent of lung fibrosis was quantified using a modified Ashcroft score and revealed there was no difference in the severity of fibrosis in wild-type mice compared with *Slpi*$^{-/-}$ animals (Figure 2d).

Slpi gene deletion exacerbates bleomycin induced weight loss but does not alter hydroxyproline deposition

It was noted that *Slpi*$^{-/-}$ mice lost more weight than wild-type mice during the acute lung injury phase of bleomycin-induced lung injury (Figure 3a). Weight loss was significantly greater in *Slpi*$^{-/-}$ mice four days post-bleomycin treatment ($P = 0.02$) and peaked five days post-bleomycin (Figure 3a). Therefore, the effect of *Slpi* gene deletion on hydroxyproline levels during the inflammatory, early and late fibrotic phases of fibrogenesis following bleomycin exposure was assessed (seven, 14 and 28 days post-bleomycin respectively). There was a progressive increase in hydroxyproline deposition during all phases of fibrogenesis in wild-type mice that reached statistical significance 28 days following bleomycin exposure ($P = <0.0001$ Figure 3b). There was also an increase hydroxyproline in *Slpi*$^{-/-}$ mice 28 days following bleomycin although the levels appeared marginally, but non-significantly, lower at each time point than in wild-type mice (Figure 3b).

Slpi gene deletion impairs *Col1α1, Col3α1* and *Col4α1* gene expression during fibrogenesis but promotes an early transient increase in *Col6α1* gene expression

Sustained expression of *Col1α1 and Col4α1* was only observed in wild-type mice, whereas in *Slpi*$^{-/-}$ mice there was a small initial rise in *Col1α1* and *Col4α1* gene expression but this did not increase during the fibrotic phase of the model and 28 days post-bleomycin levels of *Col1α1* gene expression were significantly greater in wild-type mice compared with *Slpi*$^{-/-}$ animals ($P = 0.0124$) (Figure 4a). In wild-type animals, the expression of *Col3α1* mRNA was significantly increased 28 days post-bleomycin and, again, there was no increase in *Slpi*$^{-/-}$ animals. However, an early and transient increase in *Col6α1* mRNA seven days following injury was observed in *Slpi*$^{-/-}$ animals ($P = 0.011$) (Figure 4a). Lung tissue sections, taken 28 days post-bleomycin instillation, were stained for collagen type I, III, IV and VI (Figure 4b). Collagen type I and VI positively stained tissue, in fibrotic lesions greater than 7 500 μm^2, was evaluated. Despite differences in gene expression between wild-type and *Slpi*$^{-/-}$ mice there are no differences in collagen type I and VI composition of fibrotic lesions (Figure 4c).

Discussion

SLPI is an inhibitor of protease activity and deletion of *Slpi* in mice has been associated with increased elastase activity, enhanced TGF-β activity, prolonged wound healing and increased inflammatory cell influx into wounds (19, 20). We therefore hypothesized *Slpi*$^{-/-}$ mice would have enhanced lung injury and fibrosis compared with wild-type controls. Surprisingly, despite evidence of enhanced metalloproteinase activity, more severe injury and increased *Col6α1* gene expression at early time points, we did not observe worsening fibrosis; indeed a trend towards reduced fibrosis was observed. Furthermore, we did not detect enhanced alveolar TGF-β activity following injury.

Assessment of alveolar TGF-β activation can be achieved by measuring nuclear Smad2 phosphorylation, a process specific to TGF-β signalling, in alveolar macrophages, whereas global TGF-β activity can be assessed by immunohistochemistry. Alveolar activation of TGF-β in normal lungs is primarily mediated via the αvβ6 integrin (25, 26). Wild-type mice

had a significant increase in phosphorylation of macrophage Smad2 following bleomycin supporting the important role of αvβ6 integrin mediated TGF-β activation in this model (26). Although there was a trend towards increased basal alveolar TGF-β activity in *Slpi*$^{-/-}$ mice, there was no significant increase above these higher basal levels following bleomycin induced lung injury. It is known that tethering of the latent TGF-β complex to a stiff extracellular matrix is crucial for the force generation required for αvβ6 integrin mediated TGF-β activation (27, 28). It is therefore possible that increased matrix degradation associated with reduced SLPI prevents sufficient force generation required for this mechanism of TGF-β activation. Increased pSmad2 was similarly observed in the alveoli of *Slpi*$^{-/-}$ mice at baseline consistent with the data from alveolar macrophages and data from previously published studies (19). However, even in *Slpi*$^{-/-}$ mice there was an increase in pSmad2 in the fibroproliferative lesions of mice following bleomycin. Moreover, pSmad2 levels in bleomycin treated wild-type, and *Slpi*$^{-/-}$ mice, were not different using either assessment of TGF-β activity suggesting that the effect of bleomycin on TGF-β activation, especially in mesenchymal cells, is independent of SLPI which may explain the development of lung fibrosis in animals of either genotype.

No difference in NE activity in lung homogenates from mice of either genotype or level of injury was detected. Whilst this may reflect the timing of the assay after the resolution of inflammation, at the peak of the fibroproliferative phase of the bleomycin model, it may also reflect the importance of other proteinases, such as the lysosomal cysteine proteinase cathepsin K. Cathepsin K has potent collagenolytic activity and transgenic mice over-expressing it have reduced lung fibrosis (29). Similarly *Ctsk*$^{-/-}$ mice have increased BLM-induced pulmonary fibrosis (30), and furthermore cathepsin K inhibits TGF-β generation (31). In clinical studies of osteoporosis a small number of patients treated with the cathepsin K inhibitor balicatib developed skin fibrosis (32) consistent with the pro-fibrotic effect of cysteine proteinases.

Previous studies have suggested that SLPI can inhibit MMP-9 expression, however our studies did not demonstrate any difference in total *Mmp-9* levels at the transcriptional level between wild-type and *Slpi*$^{-/-}$ mice suggesting that SLPI is required predominately to regulate post translational modification of MMP-9 in vivo, consistent with previous studies assessing oral wounds (19, 20) and the observation that neutrophil elastase can activate MMP-9 *in vivo* (24). Increased MMP-9 has been associated with both IPF (33) and experimental models of lung fibrosis (34-36). Increased MMP-9 activity promotes fibrosis through proteolysis of the alveolar epithelial basement membrane, particularly collagen IV, resulting in impaired reepithelialization and fibroblast migration into the alveolar space (34-36), and this could in part explain the development of pulmonary fibrosis in *Slpi*$^{-/-}$ mice.

Collagen deposition during wound healing is tightly regulated and dysregulation results in a fibroproliferative state (37). Our data show that there are sustained increases in *Col1α1 and Col4α1*, in wild-type animals in the first four weeks following bleomycin induced fibrosis. However, no sustained increase in *Col1α1, Col3α1 and Col4α1* were observed in *Slpi*$^{-/-}$ mice suggesting that SLPI is somehow associated with their expression in the lungs. Despite the lack of increased gene expression, there were similar levels of collagen I, III, IV and VI

deposition in the lung, assessed by immunohistochemistry. These data suggest that in *Slpi*$^{-/-}$ mice, in contrast with wild-type mice, collagen deposition may be less dependent on collagen gene expression but could occur as a result of increased post-translational modification in a protease rich environment. Collagen VI is deposited during wound healing and is transient and precedes co-localised, collagen I deposition (38, 39) and this is consistent with our data. Interestingly, in contrast with expression of *Col1a1, Col3a1 and Col4a1*, our data suggest that *Col6a1* gene expression is independently regulated.

In summary, these data suggest that *Slpi*$^{-/-}$ mice have enhanced metalloprotease activity and lung injury following bleomycin but they lack an exaggerated pulmonary fibrotic response in the first month following injury. Furthermore, SLPI deficiency impairs *Col1a1*, *Col3a1* and *Col4a1* gene expression following injury despite collagen deposition. We hypothesize that a metalloprotease rich environment promotes post-translational processing and collagen deposition resulting in lung fibrosis.

Supplementary Material

Refer to Web version on PubMed Central for supplementary material.

ACKNOWLEDGEMENTS

This work was funded by a Wellcome Trust Research Grant Number WT085350MA. *Slpi*$^{-/-}$ mice on a B6D2F1 background were kindly donated by Sharon Wahl.

This research was funded by the Wellcome Trust (project grant number 085350), and in part supported by the Intramural Research Program of the NIH, National Institute of Dental and Craniofacial Research.

List of abbreviations

(ALI)	Acute lung injury
(BAL)	Bronchoalveolar lavage
(BLM)	Bleomycin
(IPF)	Idiopathic pulmonary fibrosis
(LAP)	Latency associated peptide
(MMP)	Matrix metalloproteinase
(NE)	Neutrophil elastase
(PCR)	Polymerase chain reaction
(SLPI)	Secretory leukocyte protease inhibitor
(TGF-β)	Transforming Growth Factor-β

References

1. Maher TM, Wells AU, Laurent GJ. Idiopathic pulmonary fibrosis: multiple causes and multiple mechanisms? Eur Respir J. 2007; 30(5):835–839. [PubMed: 17978154]

2. Gauldie J, Jordana M, Cox G. Cytokines and pulmonary fibrosis. Thorax. 1993; 48(9):931–935. [PubMed: 8236078]

3. Selman M, King TE, Pardo A. Idiopathic pulmonary fibrosis: prevailing and evolving hypotheses about its pathogenesis and implications for therapy. Ann Intern Med. 2001; 134(2):136–151. [PubMed: 11177318]

4. Kinder BW, Brown KK, Schwarz MI, et al. Baseline BAL neutrophilia predicts early mortality in idiopathic pulmonary fibrosis. Chest. 2008; 133(1):226–232. [PubMed: 18071016]

5. Pham CT. Neutrophil serine proteases: specific regulators of inflammation. Nat Rev Immunol. 2006; 6(7):541–550. [PubMed: 16799473]

6. Chua F, Laurent GJ. Neutrophil elastase: mediator of extracellular matrix destruction and accumulation. Proc Am Thorac Soc. 2006; 3(5):424–427. [PubMed: 16799086]

7. Chua F, Dunsmore SE, Clingen PH, et al. Mice lacking neutrophil elastase are resistant to bleomycin-induced pulmonary fibrosis. Am J Pathol. 2007; 170(1):65–74. [PubMed: 17200183]

8. Sakashita A, Nishimura Y, Nishiuma T, et al. Neutrophil elastase inhibitor (sivelestat) attenuates subsequent ventilator-induced lung injury in mice. Eur J Pharmacol. 2007; 571(1):62–71. [PubMed: 17599828]

9. Taooka Y, Maeda A, Hiyama K, et al. Effects of neutrophil elastase inhibitor on bleomycin-induced pulmonary fibrosis in mice. Am J Respir Crit Care Med. 1997; 156(1):260–265. [PubMed: 9230758]

10. Obayashi Y, Yamadori I, Fujita J, et al. The role of neutrophils in the pathogenesis of idiopathic pulmonary fibrosis. Chest. 1997; 112(5):1338–1343. [PubMed: 9367478]

11. Hojo S, Fujita J, Yoshinouchi T, et al. Hepatocyte growth factor and neutrophil elastase in idiopathic pulmonary fibrosis. Respir Med. 1997; 91(9):511–516. [PubMed: 9415350]

12. Wang Y, Shiota N, Leskinen MJ, et al. Mast cell chymase inhibits smooth muscle cell growth and collagen expression in vitro: transforming growth factor-beta1-dependent and - independent effects. Arteriosclerosis, thrombosis, and vascular biology. 2001; 21(12):1928–1933.

13. Taipale J, Koli K, Keski-Oja J. Release of transforming growth factor-beta 1 from the pericellular matrix of cultured fibroblasts and fibrosarcoma cells by plasmin and thrombin. J Biol Chem. 1992; 267(35):25378–25384. [PubMed: 1281156]

14. Lyons RM, Gentry LE, Purchio AF, et al. Mechanism of activation of latent recombinant transforming growth factor beta 1 by plasmin. J Cell Biol. 1990; 110(4):1361–1367. [PubMed: 2139036]

15. Jenkins RG, Su X, Su G, et al. Ligation of protease-activated receptor 1 enhances alpha(v)beta6 integrin-dependent TGF-beta activation and promotes acute lung injury. J Clin Invest. 2006; 116(6):1606–1614. [PubMed: 16710477]

16. Scotton CJ, Krupiczojc MA, Konigshoff M, et al. Increased local expression of coagulation factor X contributes to the fibrotic response in human and murine lung injury. J Clin Invest. 2009; 119(9):2550–2563. [PubMed: 19652365]

17. Eisenberg SP, Hale KK, Heimdal P, et al. Location of the protease-inhibitory region of secretory leukocyte protease inhibitor. J Biol Chem. 1990; 265(14):7976–7981. [PubMed: 2110563]

18. Abe T, Kobayashi N, Yoshimura K, et al. Expression of the secretory leukoprotease inhibitor gene in epithelial cells. J Clin Invest. 1991; 87(6):2207–2215. [PubMed: 1674946]

19. Ashcroft GS, Lei K, Jin W, et al. Secretory leukocyte protease inhibitor mediates non-redundant functions necessary for normal wound healing. Nat Med. 2000; 6(10):1147–1153. [PubMed: 11017147]

20. Angelov N, Moutsopoulos N, Jeong MJ, et al. Aberrant mucosal wound repair in the absence of secretory leukocyte protease inhibitor. Thromb Haemost. 2004; 92(2):288–297. [PubMed: 15269824]

21. Ashcroft T, Simpson JM, Timbrell V. Simple method of estimating severity of pulmonary fibrosis on a numerical scale. Journal of clinical pathology. 1988; 41(4):467–470. [PubMed: 3366935]

22. Livak KJ, Schmittgen TD. Analysis of relative gene expression data using real-time quantitative PCR and the 2(−Delta Delta C(T)) Method. Methods. 2001; 25(4):402–408. [PubMed: 11846609]

23. Pezzato E, Dona M, Sartor L, et al. Proteinase-3 directly activates MMP-2 and degrades gelatin and Matrigel; differential inhibition by (−)epigallocatechin-3-gallate. Journal of leukocyte biology. 2003; 74(1):88–94. [PubMed: 12832446]
24. Ferry G, Lonchampt M, Pennel L, et al. Activation of MMP-9 by neutrophil elastase in an in vivo model of acute lung injury. Febs Lett. 1997; 402(2-3):111–115. [PubMed: 9037177]
25. Goodwin A, Jenkins G. Role of integrin-mediated TGFbeta activation in the pathogenesis of pulmonary fibrosis. Biochem Soc Trans. 2009; 37(Pt 4):849–854. [PubMed: 19614606]
26. Munger JS, Huang XZ, Kawakatsu H, et al. The integrin alpha v beta 6 binds and activates latent TGF beta 1: A mechanism for regulating pulmonary inflammation and fibrosis. Cell. 1999; 96(3): 319–328. [PubMed: 10025398]
27. Hori Y, Katoh T, Hirakata M, et al. Anti-latent TGF-beta binding protein-1 antibody or synthetic oligopeptides inhibit extracellular matrix expression induced by stretch in cultured rat mesangial cells. Kidney international. 1998; 53(6):1616–1625. [PubMed: 9607192]
28. Shi M, Zhu J, Wang R, et al. Latent TGF-beta structure and activation. Nature. 2011; 474(7351): 343–349. [PubMed: 21677751]
29. Srivastava M, Steinwede K, Kiviranta R, et al. Overexpression of cathepsin K in mice decreases collagen deposition and lung resistance in response to bleomycin-induced pulmonary fibrosis. Respiratory research. 2008; 9:54. [PubMed: 18638383]
30. Buhling F, Rocken C, Brasch F, et al. Pivotal role of cathepsin K in lung fibrosis. Am J Pathol. 2004; 164(6):2203–2216. [PubMed: 15161653]
31. Zhang D, Huang C, Yang C, et al. Antifibrotic effects of curcumin are associated with overexpression of cathepsins K and L in bleomycin treated mice and human fibroblasts. Respiratory research. 2011; 12:154. [PubMed: 22126332]
32. Runger TM, Adami S, Benhamou CL, et al. Morphea-like skin reactions in patients treated with the cathepsin K inhibitor balicatib. Journal of the American Academy of Dermatology. 2012; 66(3):e89–96. [PubMed: 21571394]
33. Selman M, Ruiz V, Cabrera S, et al. TIMP-1, -2, -3, and -4 in idiopathic pulmonary fibrosis. A prevailing nondegradative lung microenvironment? Am J Physiol Lung Cell Mol Physiol. 2000; 279(3):L562–574. [PubMed: 10956632]
34. Ruiz V, Ordonez RM, Berumen J, et al. Unbalanced collagenases/TIMP-1 expression and epithelial apoptosis in experimental lung fibrosis. Am J Physiol-Lung C. 2003; 285(5):L1026–L1036. [PubMed: 12882763]
35. Selman M, Pardo A. Role of epithelial cells in idiopathic pulmonary fibrosis: from innocent targets to serial killers. Proc Am Thorac Soc. 2006; 3(4):364–372. [PubMed: 16738202]
36. Patterson ML, Atkinson SJ, Knauper V, et al. Specific collagenolysis by gelatinase A, MMP-2, is determined by the hemopexin domain and not the fibronectin-like domain. Febs Lett. 2001; 503(2-3):158–162. [PubMed: 11513874]
37. Clarke DL, Carruthers AM, Mustelin T, et al. Matrix regulation of idiopathic pulmonary fibrosis: the role of enzymes. Fibrogenesis & tissue repair. 2013; 6(1):20. [PubMed: 24279676]
38. Oono T, Specks U, Eckes B, et al. Expression of type VI collagen mRNA during wound healing. The Journal of investigative dermatology. 1993; 100(3):329–334. [PubMed: 8440917]
39. Specks U, Nerlich A, Colby TV, et al. Increased expression of type VI collagen in lung fibrosis. Am J Respir Crit Care Med. 1995; 151(6):1956–1964. [PubMed: 7767545]

Europe PMC Funders Author Manuscripts

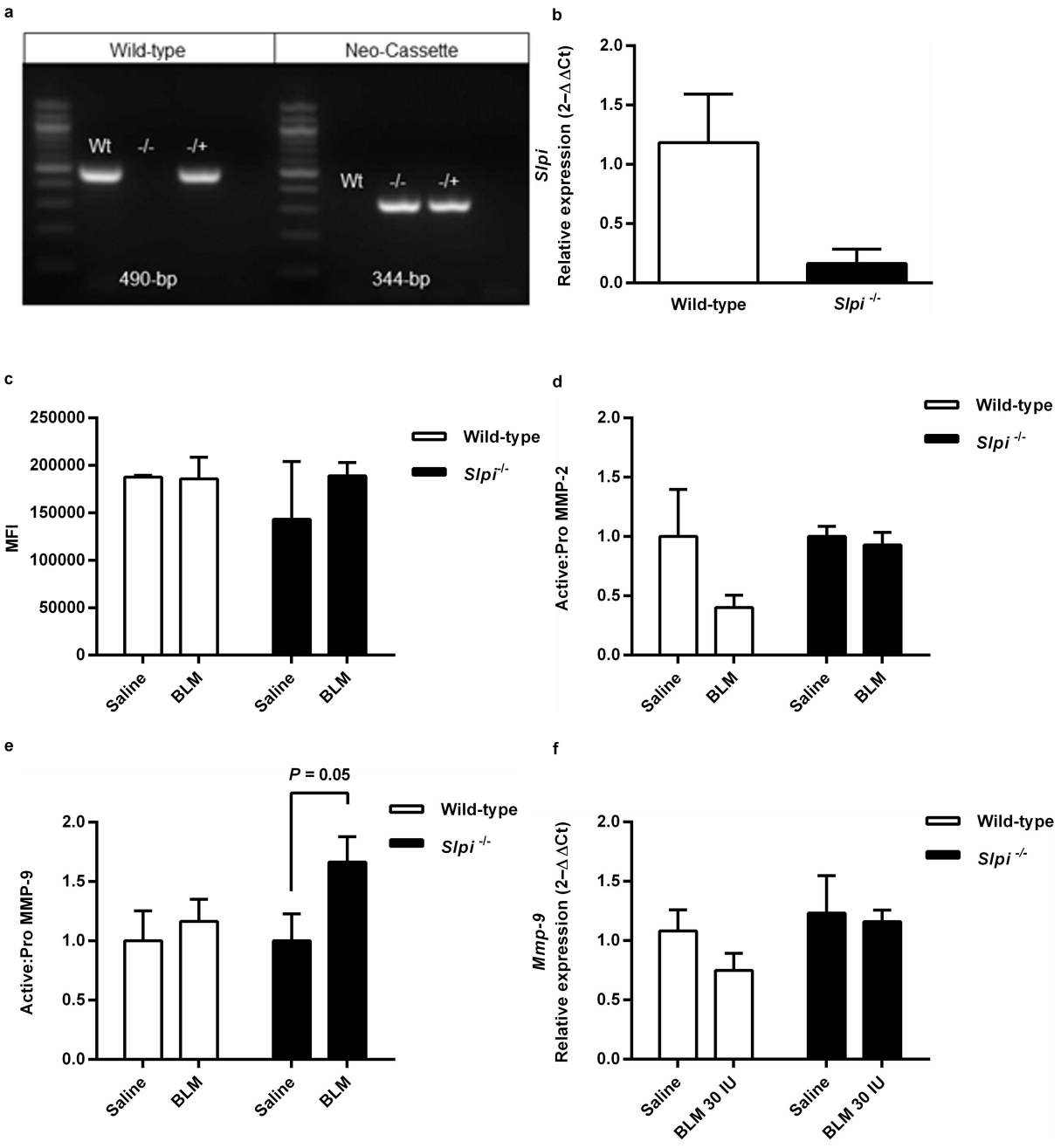

Figure 1. *Slpi*$^{-/-}$ mice do not express *Slpi* mRNA and have enhanced MMP-9 activity in the lung

(**a**) PCR confirmation of presence of wild-type 490-bp fragment and absence of Neo-cassette fragment 344-bp in wild-type animals (Wt) and absence of wild-type fragment and presence of Neo-cassette in *Slpi*$^{-/-}$ animals (−/−). Both wild-type and Neo-cassette fragments were present in heterozygous animal (−/+). (**b**) *Slpi* gene expression in lung homogenates from wild-type and *Slpi*$^{-/-}$ animals. Data expressed as mean relative expression ($\Delta\Delta C_t$) ± SEM; $n = 3$. (**c**) Neutrophil elastase activity was assessed in lung homogenate 28 days post-bleomycin treatment. Data expressed as mean fluorescence intensity (MFI) ± SEM; $n \geq 2$.

Europe PMC Funders Author Manuscripts

(**d**) Ratio of pro and active forms of MMP-2 in BAL supernatant from wild-type and *Slpi*$^{-/-}$ mice and (**e**) Ratio of pro and active forms of MMP-9 in BAL supernatant from wild-type and S*lpi*$^{-/-}$ mice. Mean ± SEM; $n = 8$. (**f**) *Mmp-9* mRNA levels in lung homogenates 28 days post-bleomycin (BLM). Data expressed as mean relative expression ($\Delta\Delta C_t$) ± SEM; $n = 8$.

Europe PMC Funders Author Manuscripts

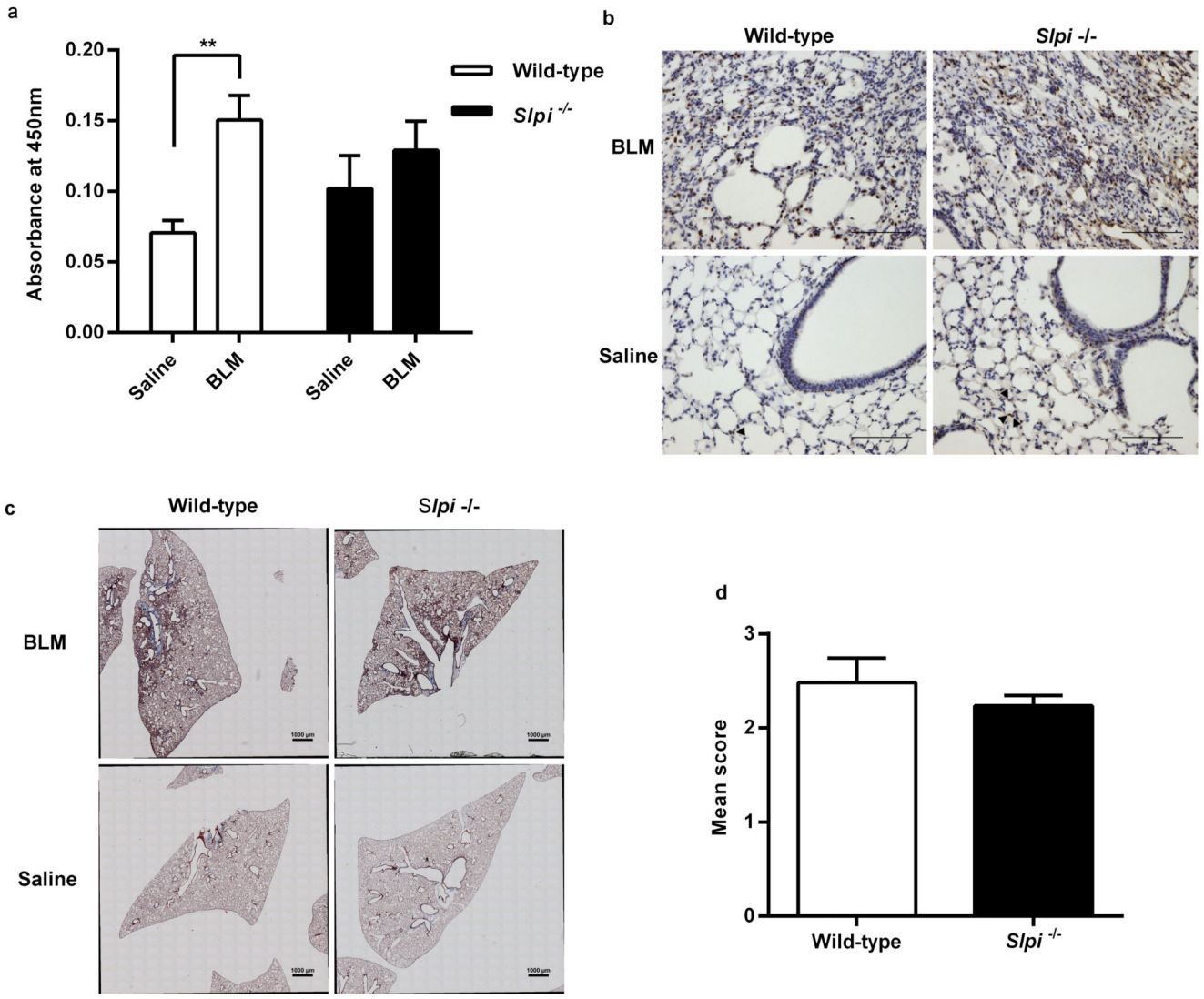

Figure 2. The effect of *Slpi* deletion on alveolar macrophage TGF-β activation and pulmonary fibrosis

(**a**) pSmad2 levels in nuclear extracts from BAL cells from $Slpi^{-/-}$ and wild-type mice 28 days post-bleomycin (BLM). Data expressed as mean absorbance at 450 nm ± SEM; $n \geq 5$; $^{**}P < 0.005$ BLM vs. saline. (**b**) pSmad2 immunohistochemistry. Representative images captured using original magnification x20, scale bars 100 μm. Arrowheads identify positively stained cells within a single, representative, alveolus in saline treated mice only; there is just one arrowhead in the wild-type mouse and three in the $Slpi^{-/-}$ mouse. (**c**) Masson's trichrome staining 28 days post-BLM treatment. Representative, whole lung lobe, cross sections. (**d**) Quantitative assessment of trichrome staining. Data expressed as mean Ashcroft Score ± SEM; $n \geq 3$.

Europe PMC Funders Author Manuscripts

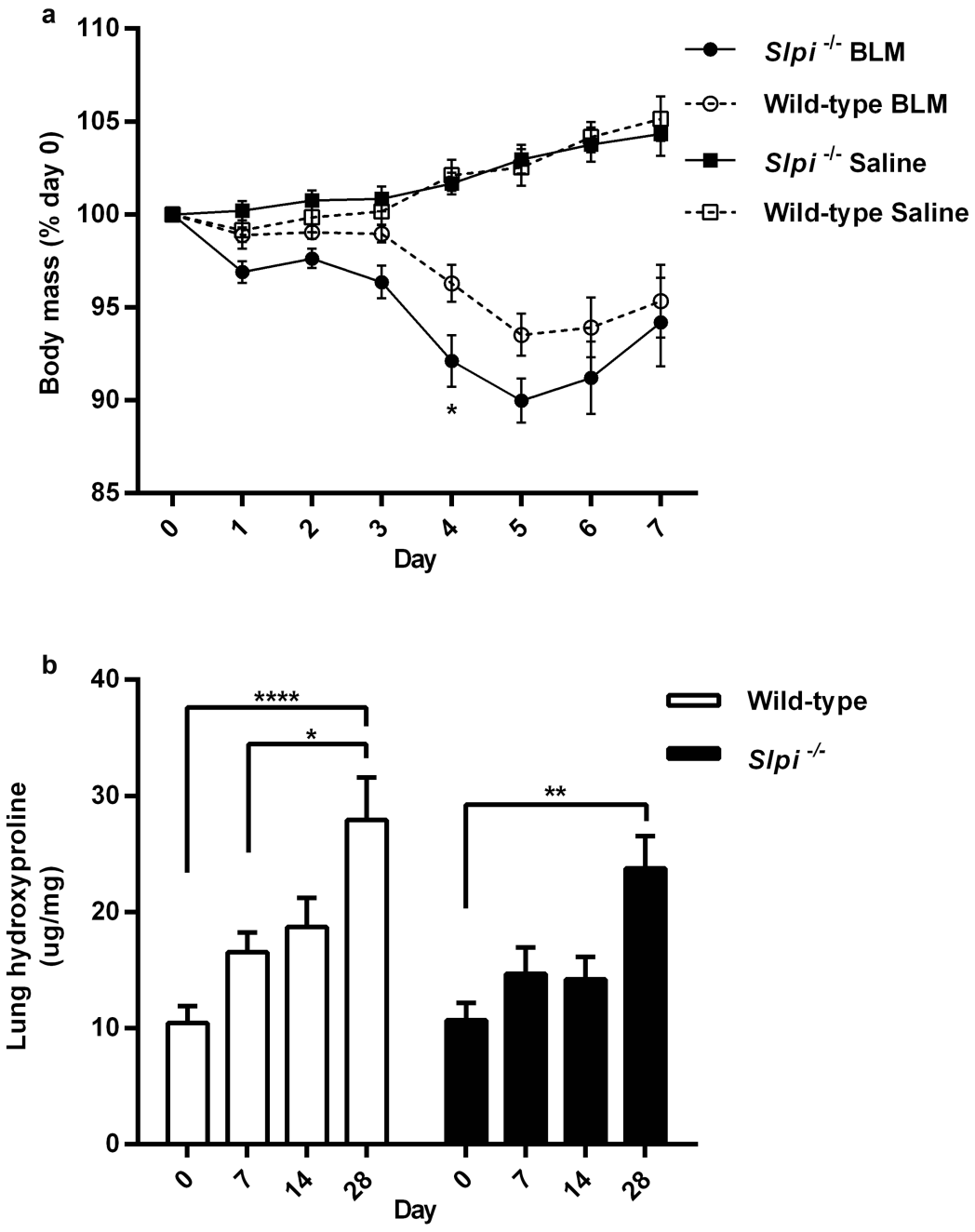

Figure 3. The effect of *Slpi* deletion on weight loss and lung hydroxyproline levels

(**a**) Body weight during the acute lung injury phase of the model in $Slpi^{-/-}$ compared with wild-type mice. Data expressed as mean percentage of initial (day 0) body mass (%) ± SEM; $n \geq 9$; Significant difference determined at day 4 $^{*}P < 0.05$ $Slpi^{-/-}$ vs. wild-type post-bleomycin (BLM). (**b**) Lung hydroxyproline levels were assessed at 0, 7, 14 and 28 days following BLM in $Slpi^{-/-}$ vs. wild-type mice. Data expressed as the amount of hydroxyproline per mg of lung tissue (μg/mg) ± SEM; $n \geq 8$. $^{*}P < 0.05$, $^{**}P < 0.01$ and $^{****}P < 0.0001$.

Europe PMC Funders Author Manuscripts

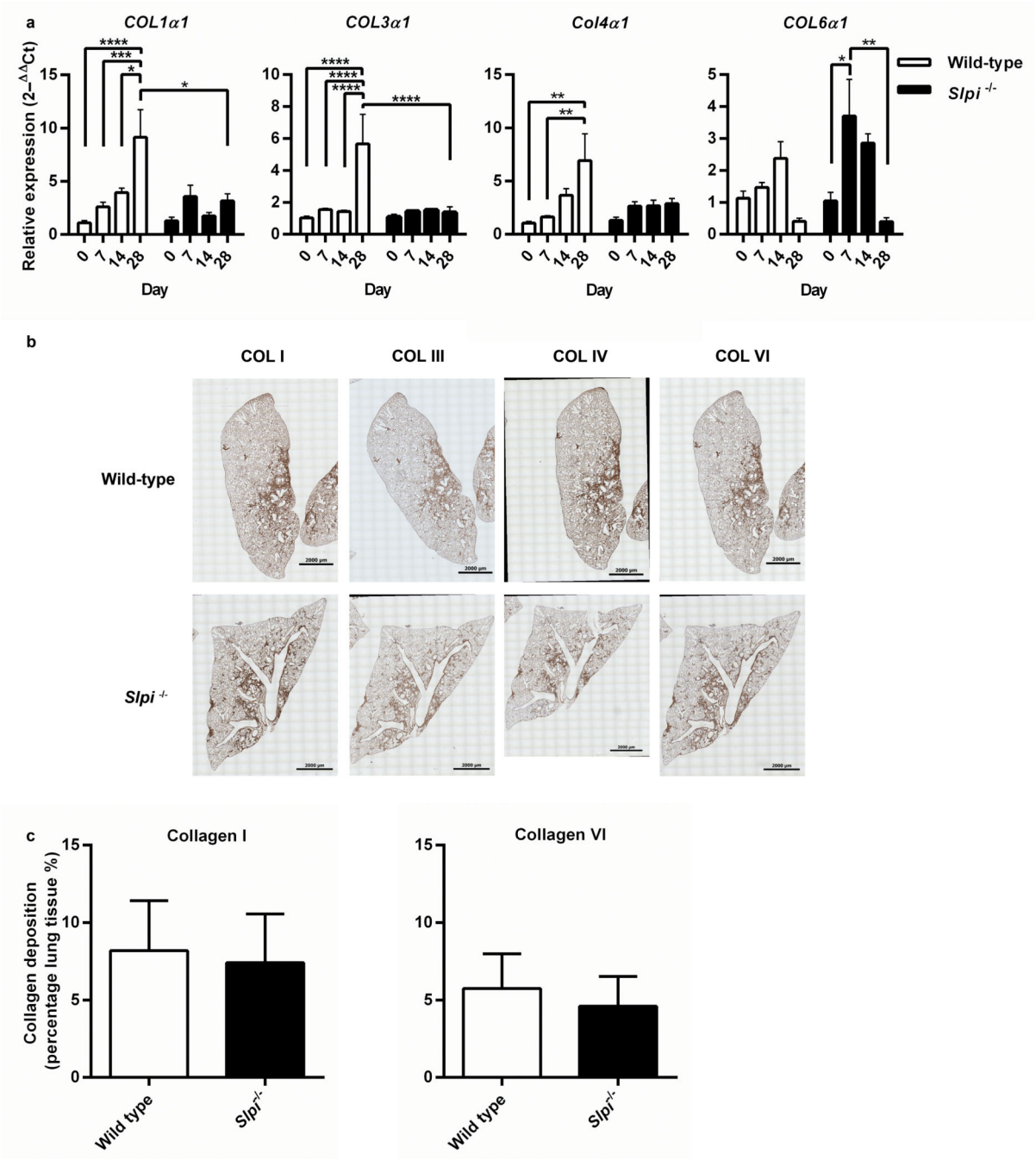

Figure 4. The effect of *Slpi* deletion on subtype specific collagen synthesis and deposition

(**a**) *Col1a1*, *Col3a1*, *Col4a1* and *Col6a1* gene expression 0, 7, 14 and 28 days post-bleomycin (BLM). Data expressed as mean relative expression ($\Delta\Delta C_t$) ± SEM; $n \geq 8$, *$P <$ 0.05, ** $P < 0.01$, ***$P < 0.001$ and **** $P < 0.0001$. (**b**) 5 μm thick tissue sections from BLM treated wild-type and $Slpi^{-/-}$ mice were stained with anti-collagen I, anti-collagen III, anti-collagen IV and anti-collagen VI. Low magnification (x10) images were stitched together to visualise whole lung lobes. Images are representative of $n \geq 3$ animals. (**c**) Collagen I and VI deposition was measured in lung tissue sections. Data expressed as mean

percentage of total lung tissue comprised of fibrotic lesions greater than 7 500 μm^2 containing collagen I and collagen VI (%) ± SEM; $n \geq 3$.

Europe PMC Funders Author Manuscripts